Experimental Inquiry into the Feasibility of Generating Laguerre-Gauss Modes at Laser Powers of Order 100W

S.M. MacKenzie *supervised by L. Carbone and A. Freise*[1]

(Gravitational Waves Group at University of Birmingham
Department of Physics and Astronomy, Birmingham UK B15 2TT)

[1] *Department of Physics and Astronomy, University of Louisville, Louisville KY 41074*

(Dated: July 29, 2011)

We present the prototype development of an experiment to test the efficacy of higher order Laguerre-Gauss modes (specifically LG_{33}) with the technology of Advanced LIGO, namely high power lasers. Before experimenting with the 200 W laser in Hanover, the optical instruments were tested in Birmingham. By replicating the beam parameters of Hanover, we were able to characterize the beam incident on and outcoming from the diffractive optical element (DOE), which created the LG_{33} mode, and a linear mode cleaner (LMC), which increased the purity of the higher-order LG beam. These results will serve as the control with which to compare the data collected in Hanover with the 200 W.

I. INTRODUCTION

Gravitational waves (GW) are the ripples in the fabric of space time caused by the movements of massive bodies predicted by Einstein's theory of general relativity. If detected, GW could provide a wealth of new information previously unattainable from electromagnetic observation alone, such as the geometry of a black hole or the mass-radius relation for neutron stars [1]. Ground based interferometers like the Laser Interferometer Gravitational Wave Observatory (LIGO) are designed to detect GW by comparing the path length of a laser beam that travels two four-kilometer-long arm cavities of an interferometer. A GW wave passing through the Earth should effectively change the optical path length of each arm in a "squeeze and stretch" motion, thus analysis of the interference of the recombined beam, having split and reflected off mirrors located at the end of each cavity and returned the the start, should reveal differences in proper length in the presence of a GW. The difficulties of detection lie in the scale of the gravitational wave signal– strong sources like violent astrophysical events will demonstrate amplitude sensitivities of up to 10^{-21}m over periods on the millisecond scale, according to most recent theoretical predictions [2].
Though LIGO and its contemporary laser interferometers have defined upper limits of detector sensitivities, GW have not yet been directly observed. The next generation of detectors, including Advanced LIGO, will employ new techniques to increase overall sensitivity. Sensitivity is limited by several factors such as seismic, mechanical, thermal, and quantum noise. This project will address improving the overall sensitivity by reducing two of these factors: combining higher-order Laguerre-Gauss modes, which reduce mirror coating thermal noise, and high power lasers, which reduce quantum photon shot noise.

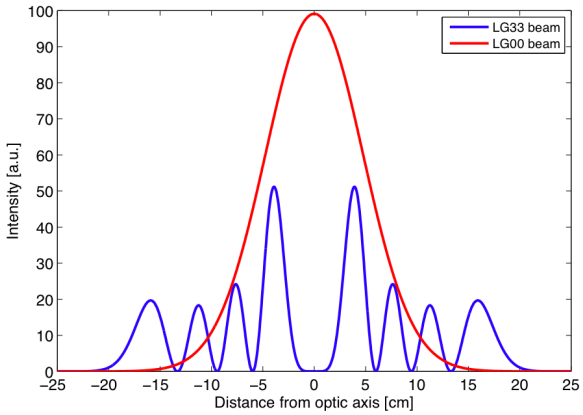

FIG. 1. A comparison of the intensity profiles of the fundamental LG_{00} and higher order LG_{33}. The wider distribution of power of the LG_{33} has been shown to reduce thermal noise.

Current gravitational wave detectors use LG_{00} fundamental Gaussian beams in their interferometers. The fundamental mode, expressed as

$$u(x,y,z) = \sqrt{\frac{2}{\pi}}\frac{1}{w(z)}\exp(i\Psi(z))\exp\left(-ik\frac{x^2+y^2}{2R_{oC}} - \frac{x^2+y^2}{w^2(z)}\right) \tag{1}$$

is a well understood solution to the paraxial wave equation, Equation 2.

$$(\delta_x^2 + \delta_y^2)u(x,y,z) - 2ik\delta_z u(x,y,z) = 0 \tag{2}$$

Since the LG_{00} mode is easy to generate and characterize, it has been advantageous to use LG_{00} modes in the complex interferometer setups of detectors like LIGO. Thermal noise arises from the internal vibrations of the mirror due to temperature. These random fluctuations interfere with the optical path length of light incident on the mirror surface, and the effect is maximized with a fundamental beam where the beam intensity is concentrated onto the mirror's fluctuating center. Thermal noise is increasingly important, as the use of high power lasers in the next generation of detectors will increase the absorption rate and therefore temperature of the mirrors. However, it has been shown [3] that higher-order Laguerre-Gauss modes which are also solutions of the paraxial equation, described by Equation 3,

$$u_{p,l}(r,\phi,z) = \frac{1}{w(z)}\sqrt{\frac{2p!}{\pi(|l|+p)!}}\exp i(2p+|l|+1)\Psi(z))\left(\frac{\sqrt{2}r}{w(z)}\right)^{|l|}L_p^{(l)}\left(\frac{2r^2}{w(z)^2}\right)\exp\left(-ik\frac{r^2}{2q(z)} + il\phi\right) \tag{3}$$

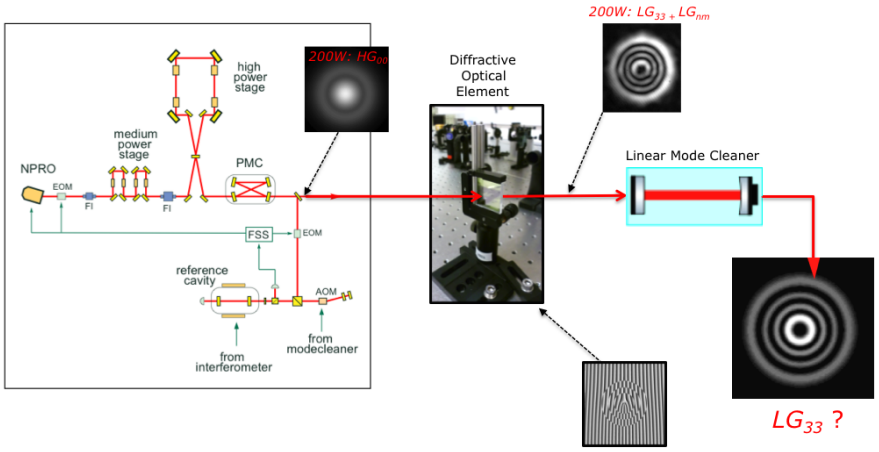

FIG. 2. Summary of project goal. The fundamental beam that exits the Hanover PMC will be fed through a diffractive optical element to create LG_{33} modes. The LG_{33} beam will then pass through a linear mode cleaner to increase the beam purity.

, can be used to reduce thermal noise. LG_{33} beams reduce the magnitude of thermal aberrations of the optical components within interferometers due to the wider distribution of beam intensity across the surface area of the mirrors upon which the beam is incident [4]. With a wider distribution, the unpredictable fluctuations are averaged out better than if the beam were to hit in a concentrated spot as with a fundamental beam. This is can be seen in Figure 1, where the intensity profiles of the LG_{00} and LG_{33} are plotted. LG_{33} beams are also the most advantageous over other proposed methods of reducing thermal noise of the laser beam as the higher-order LG beams would be compatible with the currently used spherical mirrors [5], whereas other beam shapes with wide intensity distributions like "flat" and "Mexican hat shaped" beams are not [5]. Thus, using LG_{33} beams would increase the sensitivity of future gravitational wave detectors while reducing the need for thermal compensation systems [5].

One aspect of quantum noise is the photoelectron shot noise, the fluctuations in the photocurrent signal that arise from the uncertainty of interferometer's laser field. Quantum fluctuations affect the number of photons able to be detected and the error in detecting photons gets smaller compared to the absolute number with increased number of photons incident on the substrate [2]. Therefore, since we assume the photoelectrons to follow a Poisson distribution, where the signal-to-noise ratio (SNR) is dependent on the number of photons, N,

$$\mathrm{SNR} \propto \frac{\sqrt{\mathrm{N}}}{\mathrm{N}} \propto \frac{\sqrt{\mathrm{LaserPower}}}{\mathrm{LaserPower}} \tag{4}$$

the SNR for shot noise can be improved by increasing the number of photons, i.e. increasing the laser power [6]. It is interesting to note another kind of quantum noise, radiation pressure noise, thought to originate from the uncertainty in how the beam splitter divides the high power beam between the two arm cavities [2]. Radiation pressure noise increases with higher laser power, while shot noise decreases, setting an overall sensitivity limit known as the Standard Quantum Limit (SQL). It has been proposed to bypass the SQL by installing Fabry-Perot cavities in the arms to filter the output signal [2].

The combination of higher order Laguerre-Gauss modes and high power laser beams should work to increase GW detector sensitivity by decreasing the effects of thermal and shot noise. However, though each has been independently investigated to determine effectivity and feasibility [5, 6], it is still necessary to prove experimentally that higher order Laguerre-Gauss modes and high power lasers are realistically compatible with each other, for instance in case of the Advanced LIGO 200 W laser. In collaboration with the Advanced LIGO group in Hanover [, **?** , wilke] the Gravitational Waves Group at the University of Birmingham is investigating the generation of LG_{33} modes at high power lasers and related technologies necessary in future detectors. The goal of this experiment, summarized in Figure 2, is to pick off the 200 W laser beam after the pre-mode cleaner in Hanover, pass this fundamental beam through a diffractive optic element to create an LG_{33} beam, then feed the beam through a linear mode cleaner to analyze the purity of the LG_{33} beam. Before testing LG_{33} modes directly with the Advanced LIGO 200W laser, we test the experimental set-up in Birmingham to ensure practical methodology. The experiment in Birmingham will then be integrated into the Hanover prototype setup to investigate LG_{33} mode behavior with the 200 W laser. This is done by replicating the Hanover beam (same wavelength, beam waist, and beam position), installing a diffractive optical element to create an LG_{33} beam, characterizing the LG_{33} beam, manufacturing a linear mode cleaner (LMC) as in [5], installing the LMC into the system, and finally characterizing the beam purity after the LMC.

II. EXPERIEMENT

A. General properties of Gaussian Beams

The properties of Gaussian beams are described with the following parameters. The Rayleigh range is an approximation of the length of the near-field region (the area around the beam waist) and is given by

$$z_R = \frac{\pi\omega_0^2}{\lambda}. \tag{5}$$

The Rayleigh range is related to the beam waist at a given position z by

$$\omega(z) = \omega_0\sqrt{1 + \left(\frac{z - z_0}{z_R}\right)^2}. \tag{6}$$

The Gaussian beam parameter q describes the interaction of Gaussian modes with optical components. This complex quantity is expressed as

$$q(z) = iz_R + z - z_0 \tag{7}$$

where z_0 is the position of the beam waist and z is the position of calculation. The real part of q is used to calculate the beam's radius of curvature from the relation

$$R_{oC} = \frac{1}{\text{Real(q(z))}} \tag{8}$$

while the imaginary part is related to the beam waist w_0,

$$w_0 = \sqrt{i\left(\frac{\lambda\pi}{q_0}\right)^{-1}}. \tag{9}$$

Any beam is uniquely defined by wavelength, beam waist size, and beam waist position (thus the beam parameter depends on these three variables only). This allows us to recreate the Hanover beam profile by maintaining ω_0, z_0, and λ in our Birmingham setup.

B. Replicating the Hanover Beam Profile

The Advanced LIGO Laser shown in Figure 3 is composed of a non-planar ring oscillator, a 35 W amplifier, and an injection-locked high-power oscillator. The 200 W output power can be locked by a control loop feeding to a piezoelectric actuator. A detailed characterization of the laser and a description of the stabilization techniques are available in [6]. The beam that enters our system comes directly from the pre-mode cleaner (PMC) of the Advanced LIGO setup, which is used to reduce the higher-order mode content of the laser beam for a collimated fundamental mode beam. From exiting the PMC, the beam of the Advanced LIGO setup has a beam waist of 547 μm. Thus, to prepare the Birmingham setup in which we test our LG_{33} modes and linear mode cleaner we must have an incoming beam with the same beam waist. To replicate these parameters, two lenses were placed in our arm of the Birmingham laser setup, BL-A (nominal focal length of -200 mm) and BL-B (nominal focal length of +200 mm) in Figure 4.

Figure 5 shows the beam profile of beam after BL-A and BL-B, which replicate the Hanover requirement, and after the first turning mirrors which guide the beam into the area of our Birmingham table top corresponding to the available space in Hanover. It is important to note that the positions for the BL-A and BL-B beam sizes are independent of zero we will later define from the Hanover beam's waist position, for these lenses will not be a part of the experiment in Hanover and are simply to replicate the beam conditions. The astigmatic nature of the Birmingham laser is also evident in these plots from the difference between the horizontal and vertical beam sizes.

C. Generating an Optimal LG_{00} Mode onto the DOE

1. DOE properties and requirements

Diffractive optical elements (DOE) have been shown to create higher-order Laguerre-Gaussian beams of reliable purity [8] and are compatible with high power lasers. Thus, with a high conversion efficiency (the ratio of power of the

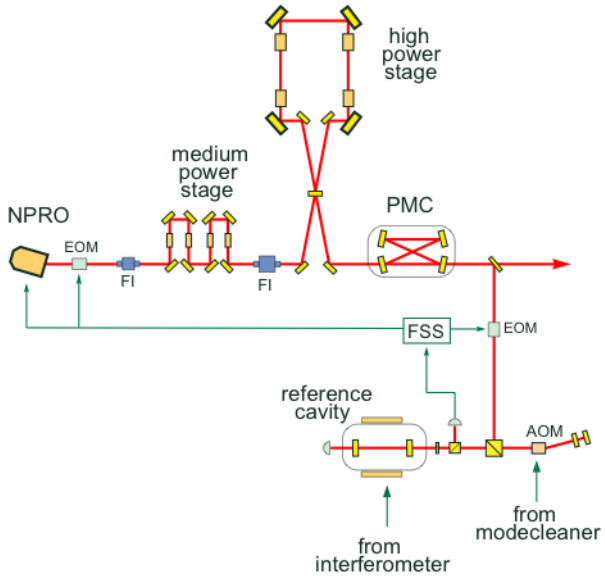

FIG. 3. Layout of the Advanced LIGO prototype in Hanover, taken from [**?** , wilke] Our experiment will concern the beam that exits the PMC with a waist of 547 μ m.

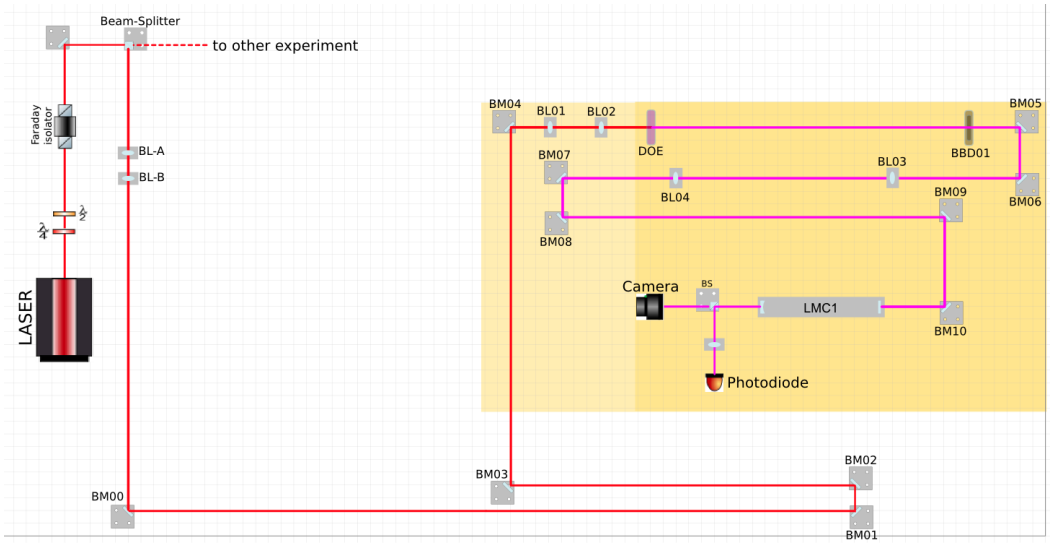

FIG. 4. Birmingham setup with relative distances to scale. BL-A and BL-B transform the Birmingham laser beam to the Hanover requirement of 547 μ m. The orange shaded area is the alloted space that will be available on the Hanover table top. The laser beam, defined in red, is of the fundamental mode before hitting the DOE. The exiting beam is imprinted with LG_{33}, differentiated by the pink beam. The 'x' marks the location equivalent to the Hanover beam waist. BMs are steering mirrors, BL are lenses, and BBD are beam dumps.

incident fundamental beam to that of the output power of our desired LG_{33} beam) and limited only by the resolution of the etching technique, a DOE is the best option for creating LG_{33} modes in our setup. A DOE is made from a glass plate etched with small scale structures with photolithographic techniques. A fundamental laser beam wave incident upon the etched glass will then be diffracted by the microstructures. The superposition of these different wave fronts propagate as the desired higher-order mode. Our DOE is optimized for 3.5 mm, collimated beam. These parameters were determined by the particular phase pattern, a spiral phase variation, designed by the University of Birmingham Gravitational Waves Group to produce the LG_{33} modes.

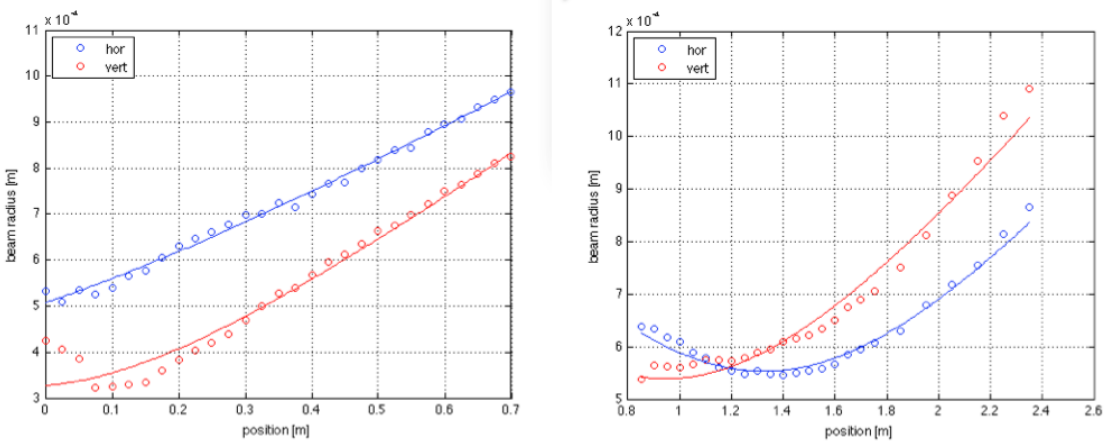

FIG. 5. Beam profile for beam created by BL-A and BL-B to replicate the Hanover conditions on the left and the beam profile in the near field of the beam entering our alloted area (shown in orange in Figure **??**. For both profiles, the data and fit for the horizontal are in blue while the vertical is in red.

2. *Analytical Calculations*

To optimize the location of the pair of lenses (BL01 and BL02) used to create a very large collimated beam in preparation for the DOE, a MatLab script was written to calculate the resultant beam parameters for changing relative distances of the lenses. These calculations were done using the ABCD matrix method, as described in [7], keeping in mind our experiment's requirements: a beam of radius 3.5 mm for optimal DOE output and the inability to install any instrument before 2 m in order to fit the Hanover space constraints. A summary of this method is given here.

One can determine q after a series of optical components, and thus easily calculate the radius of curvature and beam radius at any point. The coefficients of the matrix

$$M = \begin{bmatrix} A & B \\ C & D \end{bmatrix} \tag{10}$$

can be used to solve for the resulting q

$$\frac{q_2}{n_2} = \begin{bmatrix} A & B \\ C & D \end{bmatrix} \begin{bmatrix} \frac{q_1}{n_1} \\ 0 \end{bmatrix} \tag{11}$$

where n_2 and n_1 are the indices of refraction for the final and initial materials. In our experimental setup, both n_2 and n_1 have the value of one (index of refraction of air). Different substrates are described by different ABCD matricies. For our purposes (determining the beam parameter for the first set of lenses, one diverging and one converging), it was necessary to consider transmission through a lens and transmission through a free space. The matrix for a lens is

$$M_{lens} = \begin{bmatrix} 1 & 0 \\ -\frac{1}{f} & 1 \end{bmatrix} \tag{12}$$

and for a free space is

$$M_{free} = \begin{bmatrix} 1 & \frac{L}{n} \\ 0 & 1 \end{bmatrix} \tag{13}$$

where f is the focal length of the lens, L is the length of the free space, and n is the refractive index of the free space. With Equation 12 and Equation 13, one can trace the Gaussian beam through the optical system by multiplying together the matrices as the system requires.

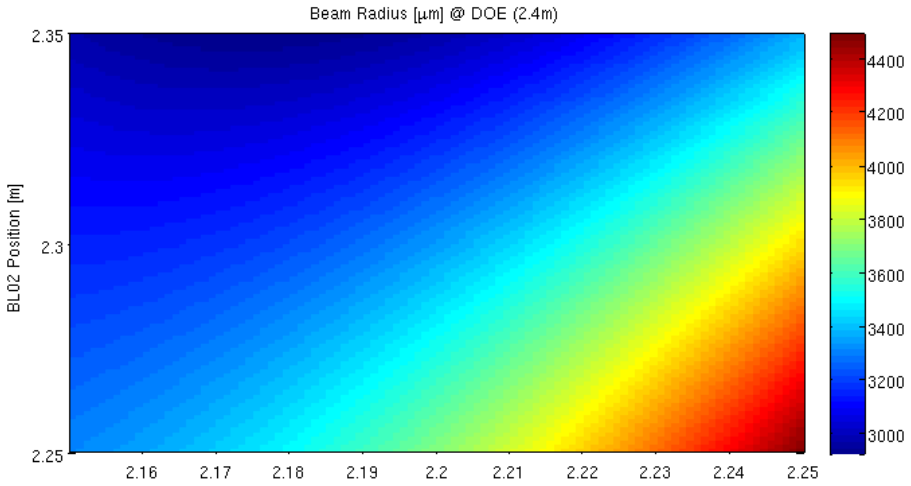

FIG. 7. (color online) Calculated beam radii for relative BL01 and BL02 positions in the Birmingham setup. The desired beam radius at the DOE is 3.5 mm, thus the light blue line indicates the desired lens positions.

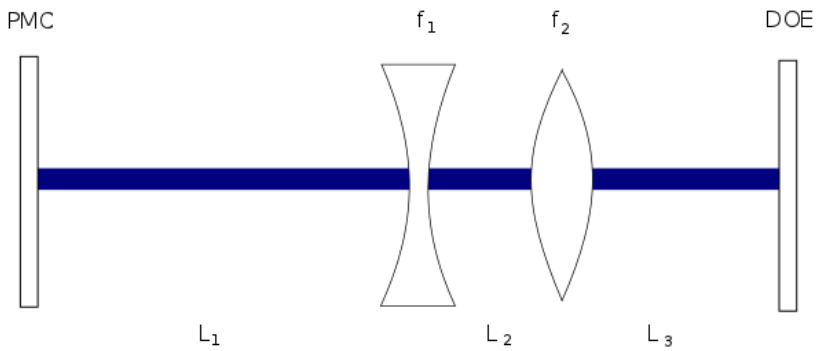

FIG. 6. Beam path through three free spaces and two lenses. The accompanying MatLab script can be adapted for the same setup with different focal lengths.

For example, the part of our system under investigation, the two lenses put in place before the DOE shown in Figure 6, our ABCD matrix looks like

$$q_{atDOE} = \begin{bmatrix} 1 & L_3 \\ 0 & 1 \end{bmatrix} \begin{bmatrix} 1 & 0 \\ -\frac{1}{f_2} & 1 \end{bmatrix} \begin{bmatrix} 1 & L_2 \\ 0 & 1 \end{bmatrix} \begin{bmatrix} 1 & 0 \\ -\frac{1}{f_1} & 1 \end{bmatrix} \begin{bmatrix} 1 & L_1 \\ 0 & 1 \end{bmatrix} \begin{bmatrix} q_{afterPMC} \\ 0 \end{bmatrix} \tag{14}$$

where all the indices of refraction are equal to one.
By creating a MatLab script for this matrix method, the initial parameters (lens focal lengths, lens substrate, etc) can be adjusted for different systems by adjusting the input values. The optical setup can also be easily modified with the inclusion of different matrices. A sample of the output of this script is shown in Figures 7 - 8, where the calculations were performed for the BL01 and BL02 lenses (see Figure 4).
To ensure the best quality beam output from the DOE, the incident beam upon the DOE's etched surface should be a well collimated beam with a radius of 3.5 mm. According to Figure 7, the optimal relative positions of BL01 and BL02 to obtain such a radius are highlighted in light blue. The almost linear relationship gives us an idea of where to initially place the lenses before allowing for fine alignment. For a well collimated beam, the radius of curvature should approach infinity, i.e. the beam front would be "flat". In Figure 8, the MatLab script calculations give that a particular linear relationship between the BL01 and BL02 lens positions yield the desired value. Outside of this relationship, the radius of curvature quickly goes to zero. The output beam from the DOE should have a beam waist of 370 μm for optimal incidence on the linear mode cleaner. Figure 9 indicates that there is a linear relationship between the two lens' position which gives this value, shown in dark red. This output beam's waist must be at a

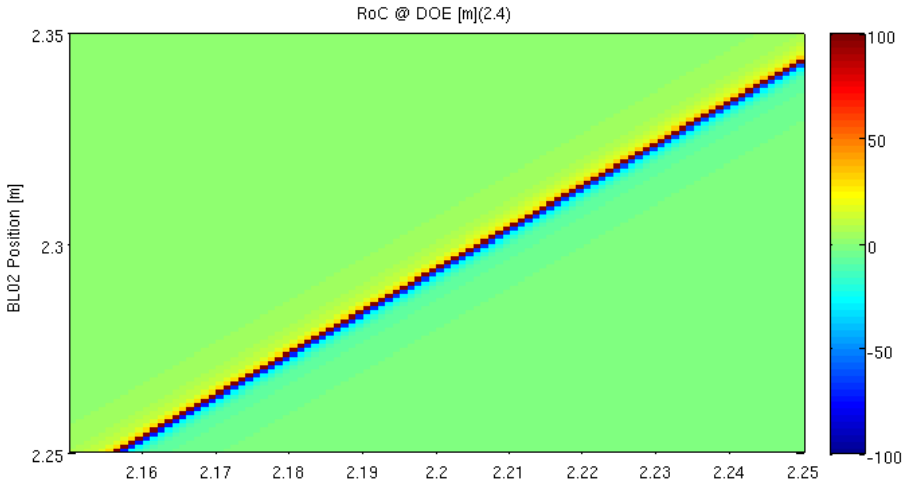

FIG. 8. (color online) Calculated radii of curvature for relative BL01 and BL02 positions in the Birmingham setup. Well collimated beams have a radius of curvature of infinity, which is seen in this graph as the red/blue line.

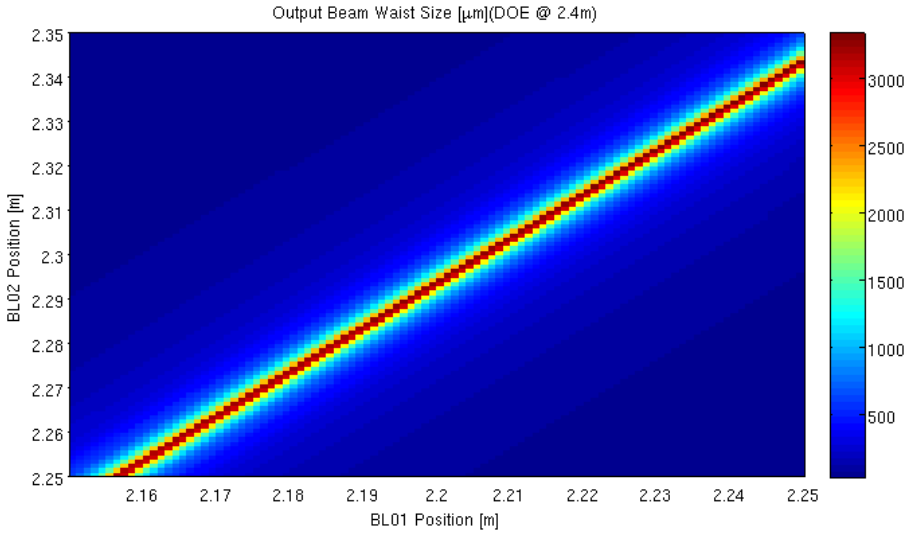

FIG. 9. (color online) Calculated beam waist size for relative BL01 and BL02 positions in the Birmingham setup. The desired output beam after the DOE should have a beam waist of 370 μm for the linear mode cleaner.

sensible distance, for a linear mode cleaner will be placed at that position. Thus, it is necessary to remember the available geometry of the Hanover setup and place BL01 and BL02 in such a position as to put the beam waist after the DOE at a convenient location. We determine that a range between three and five meters is acceptable; this corresponds to the light blue-green side of the solid line in Figure 10. The accuracy in location on the Birmingham bench is limited to increments of 2.5 centimeters, but Figures 7 - 10 show that adjustments of position on the order of one centimeter make a noticeable difference in the beam output. Therefore, though each graph gives an idea of where BL01 and BL02 should be placed in relation to each other, we expected the necessity of making alignment procedures for optimal beam output.

This mathematical analysis was verified using JamMt, an optics simulation tool with graphical interface [1]. Figure 11 shows a screen shot of the applet, where one can easily get an idea of how changes in relative lens position affect the output beam waist size and position. After installation and alignment, BL01 was located at 2.20 m and BLO2 at 2.30

[1] A. Thring and N. Lastzka, http://www.sr.bham.ac.uk/dokuwiki/doku.php?id=geosim:jammts[]=jammt

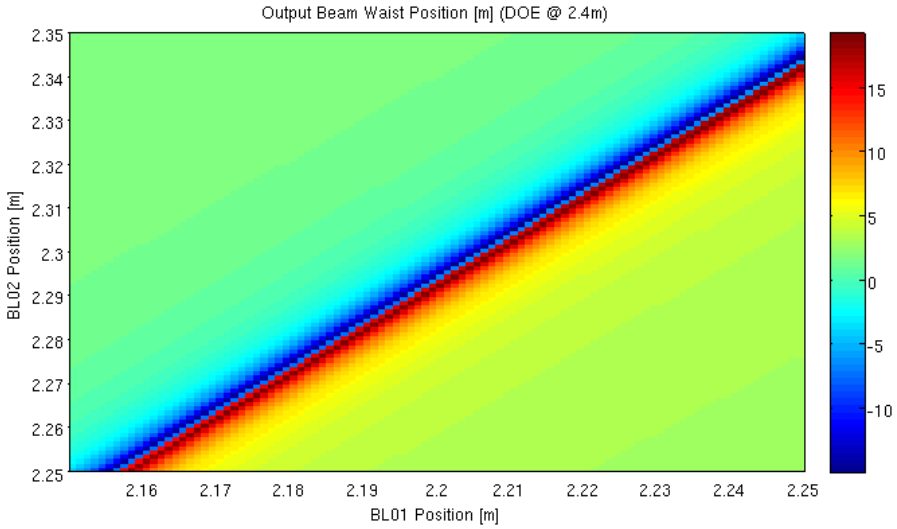

FIG. 10. (color online) Calculated beam waist position for relative BL01 and BL02 positions in the Birmingham setup. To fit the linear mode cleaner into the available space of the Hanover setup, we do not want a beam waist position too far after or too near the DOE.

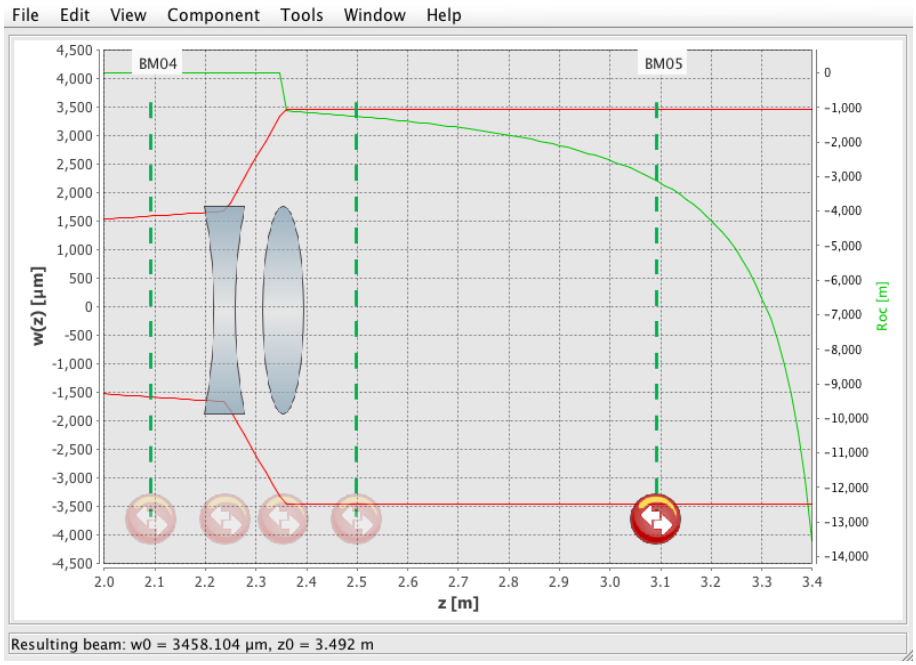

FIG. 11. Screenshot from the JamMt optics simulation applet.

m.

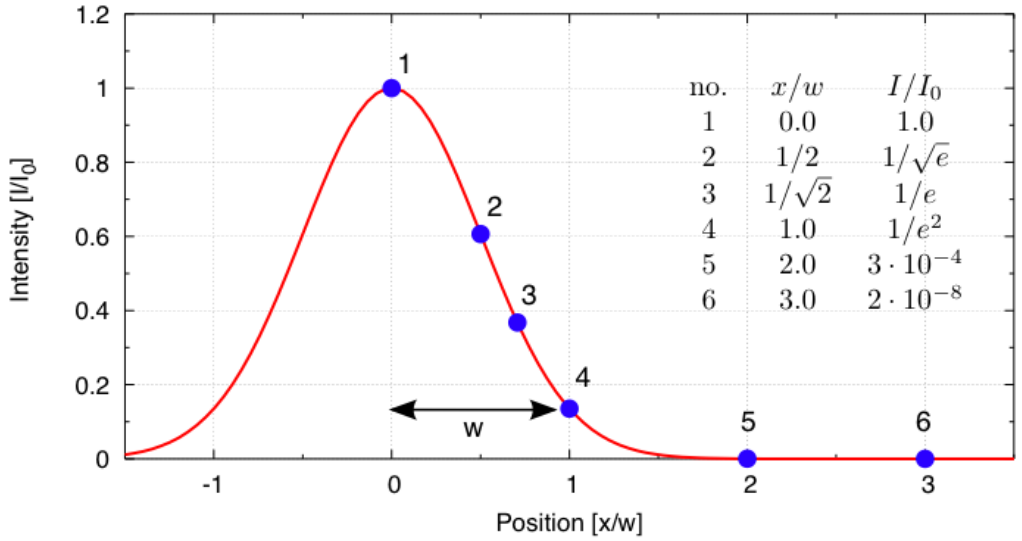

FIG. 12. One dimensional cross-section of a Gaussian beam, taken from [7].

3. *Experimental Measurements*

The measurements of beam size, displayed in Figures 5 and 13 were calculated from measurements taken at incremental positions to the optical instruments in question with a WinCamD CCD camera[2]. The WinCamD detects the intensity of a beam incident upon its lens by recording the charge accumulated from incoming photons across a surface of pixels. This data was used to plot the beam size along its path in the horizontal and vertical planes. From the beam size, a routine calculated the beam waist and beam waist position. Because the beam incident on the WinCamD was so large, the DataRay software[3] used to record the radius values for the horizontal and vertical parts of the beam could only record the value at half the power intensity instead of the desired $\frac{1}{e^2}$ fraction. (This fraction corresponds to 13.5% of the integrated power intensity.) However, it is easy to calculate this 13.5% value from the 50% data recorded by DataRay using the equation

$$\omega_{13.5\%} = \frac{\omega_{50\%}}{\sqrt{\left(\frac{log(2)}{2}\right)}} \tag{15}$$

The relationship between these two intensities is shown in Figure 12. These beam sizes were plotted against position to track the beam profile and are displayed for the horizontal beam and the vertical beam in Figures 5 and 13. The data are displayed in dots, while the lines are a result of the MatLab function FT_fit_beam_size. This function is from the SimTools[4] package, a collection of MatLab scripts and functions developed by Andreas Freise. Several iterations of this method were done in the process of aligning the optics for optimal output.

4. *Mode Matching for the DOE*

A series of measurements taken in the same manner as described above were taken after installing two lenses: BL01, a diverging lens with focal length -103.3 mm, and BL02, a converging lens with focal length 206 mm. The size was calculated for the 13.5% power intensity from the 50% as described above. A series of measurements were taken, the results were analyzed using the beam profiling method described above, then the lenses were adjusted in search of the

[2] DataRay Inc. http://www.dataray.com/
[3] DataRay Inc. http://www.dataray.com/
[4] Available for download from www.gwoptics.org

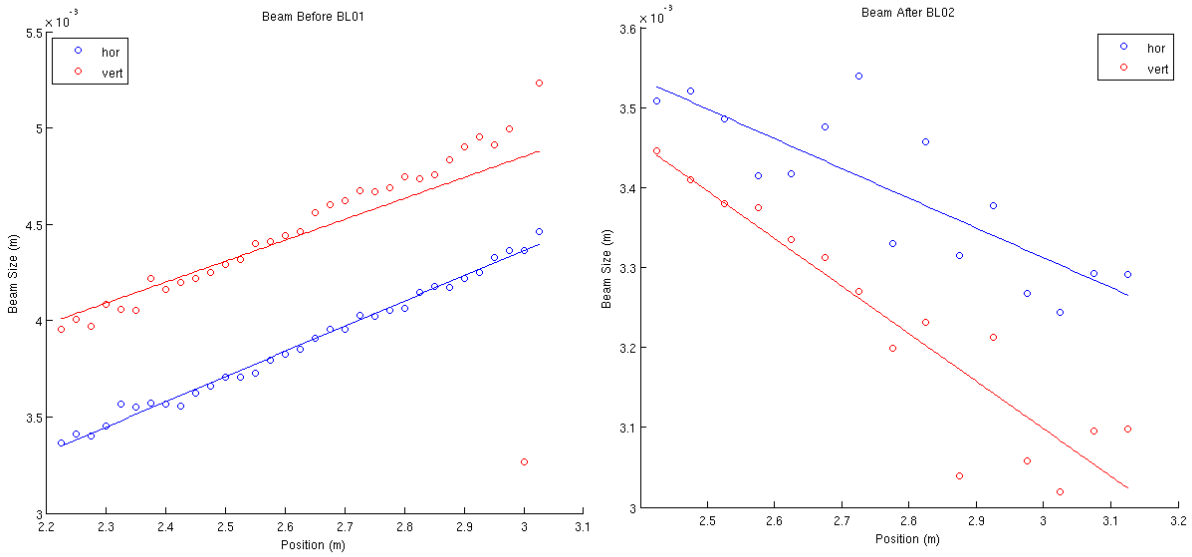

FIG. 13. Beam size measurements before (left) and after (right) BL01 and BL02 in the horizontal (blue) and vertical (red). The calculated beam waist and position after the lens of the horizontal beam are ω_0= 878.67 μ and z_0 = 11.2845 m. For the vertical beam, ω_0=560.55 μm and z_0 = 8.0430 m. Beam sizes were calculated from 50% intensity.

optimal beam. Figure **??** shows the beam before the lenses (left hand side plot) and the final beam measurements made (right hand side plot), for the beam is very large and slowly converges, fitting our requirements for the DOE. The beam size produced is not exactly 3.5 mm, but with such a large beam waist, the collimated beam will slowly converge at the desired DOE position.

D. Installation of the DOE

1. *Beam Profiling Techniques*

For optimal output, it is necessary to have a large, collimated beam centered upon the DOE. To ensure that the intensity of the incident beam is evenly distributed across the surface of and aligned along the same path axis of the DOE, a series of WinCamD pictures were taken at incremental distances, then analyzed using a fitting routine that utilizes a number of functions and scripts from the SimTools package to fit LG helical modes. Because this routine uses a method similar to the center of mass method for determining the centre, the accuracy of the generated centre guess is a good indicator of whether or not our beam is centered on the DOE.

$$x_0 = \frac{\Sigma x_i I_i}{\Sigma I_i} \tag{16}$$

Equation 16 calculates the centre position x_0 from the intensities I at given positions. Using the guessed centre and radius, the routine then does a chi-squared minimization to calculate the beam waist and beam size and fit the WinCamD data. Figure 14 shows a sample of the fitting output of this routine, taken from profiling the beam output after the DOE. The first column of plots, labeled 'data and fit', show the routine's fit overlaid upon the original WinCamD data, whereas the 'fit plots' show a calculation of the fitted beam alone. The column of 'residual' plots is the difference between the real data and the beam calculated from the fit and is quite useful–one can quickly determine if the beam is relatively aligned (little residual) or not (drastic residual).

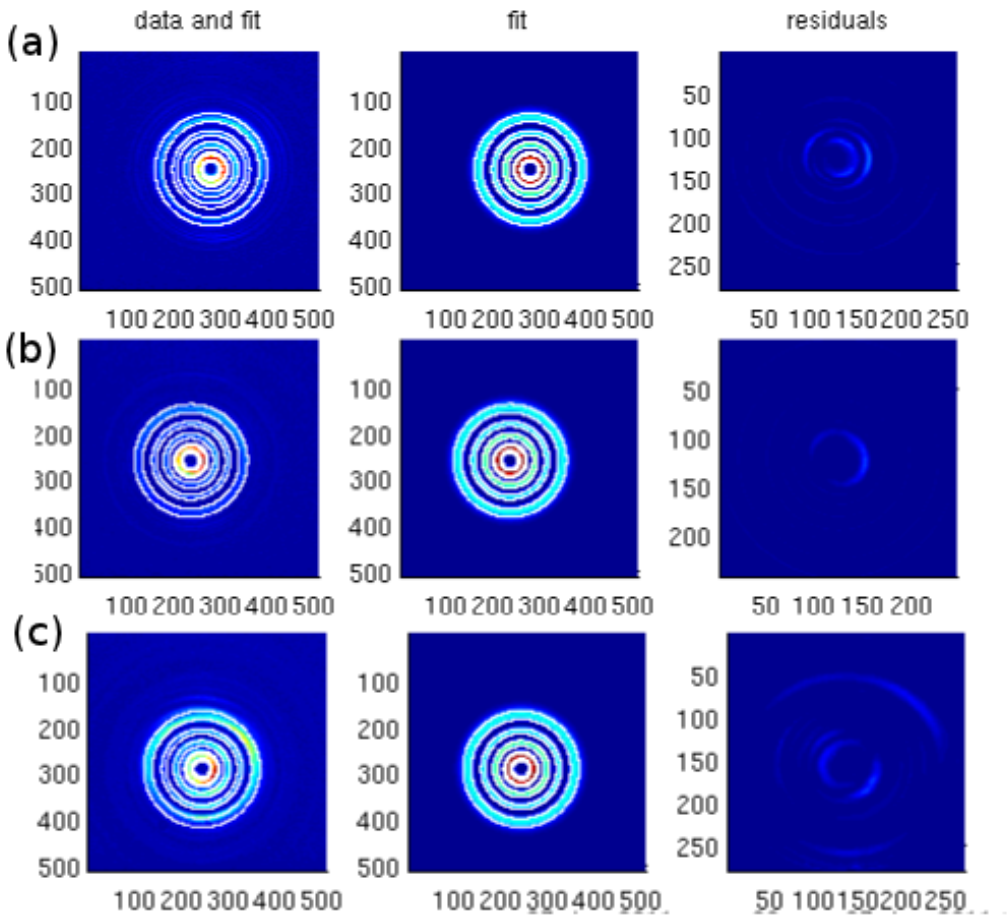

FIG. 14. A sample of output from the fitting routine for the beam after lens BL04 at (a) 3.975 m, (b) 4.005 m, and (c) 4.440 m. This routine, besides giving an idea of the helical nature of the beam, is useful as a centering tool, as one can determine quickly from the residual plots whether the beam is aligned or not.

2. Profiling the DOE Output Beam

A MatLab fitting routine was used to calculate the centre of the LG33 beam from the WinCamD files, as described in section II C 3. The accuracy of the fit's center to the beam's center indicated whether the DOE was correctly aligned, and therefore producing the optimal beam. Figure 15 shows four beam intensity profiles with the routine's centre guesses indicated by black dots. The beam exiting the DOE is profiled in Figure 16.

E. The Linear Mode Cleaner

Mode cleaners are used to ensure the purity of the laser beam. In general, they work to increase beam purity by selecting only certain modes from the beam by limiting the resonant frequencies within the mode cleaner cavity [5]. Though triangular mode cleaners have been recently favored in gravitational wave detector designs, the geometry of the cavity, which makes it highly beneficial for use with LG_{00}, renders the set-up ineffective for higher order LG modes. This is because triangular cavities produce a beam that is mirrored around the vertical axis after one full round trip. Though LG_{33} modes are symmetric around the vertical axis, they are often asymmetric in the phase cross sections. Thus, the light fields cannot constructively interfere to become fully resonant within the cavity. Also, in triangular mode cleaners a beam hits the spherical mirrors at an angle, breaking the azimuthal symmetry. Since LG_{33} modes are not eigenmodes of astigmatic cavities, unlike the fundamental LG mode, the beam will degenerate

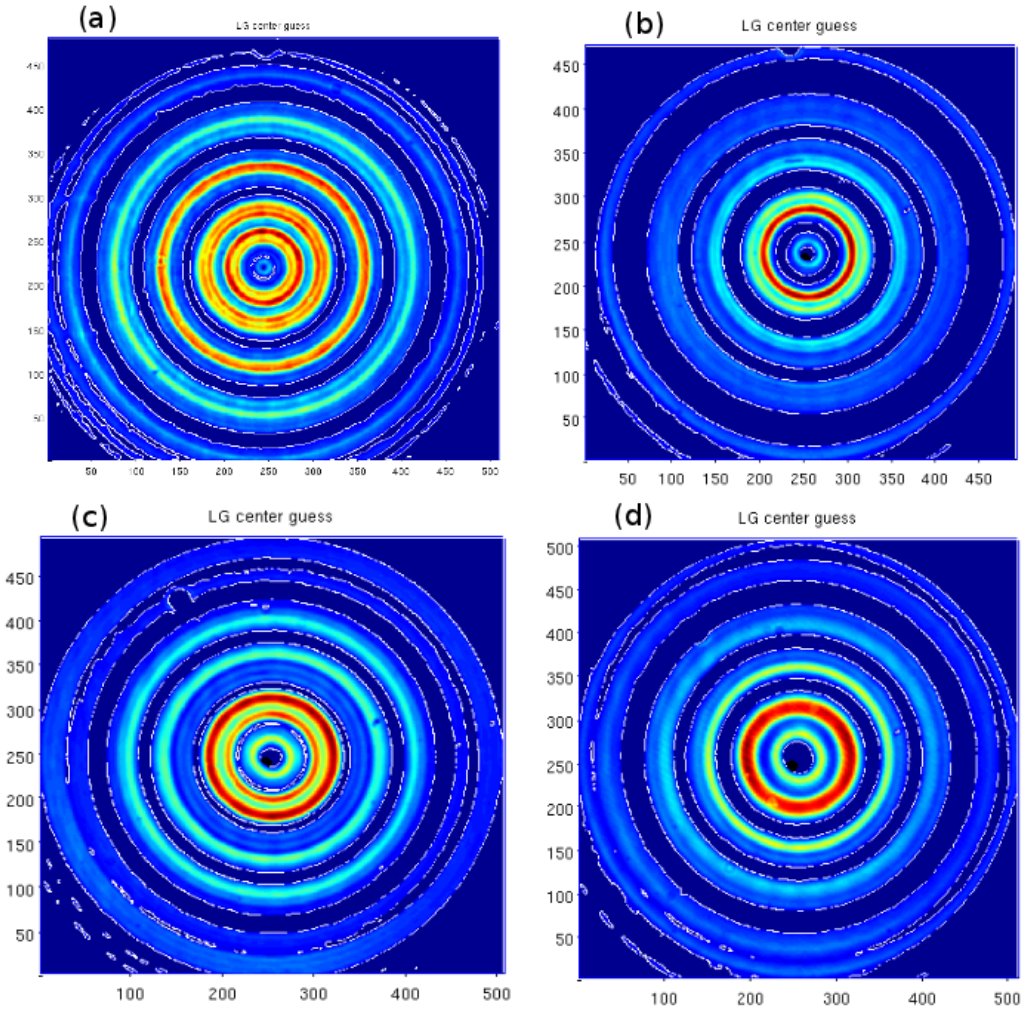

FIG. 15. Four sample intensity profiles of the beam after the DOE at (a) 2.525 m, (b) 2.795 m, (c) 2.950 m, and (d) 3.150 m. The fitting routine's guess for the beam centre are indicated by a black dot.

as a result of this astigmatism. Longitudinal control of a linear mode cleaner cavity at resonance for LG_{33} modes has already been demonstrated [5] at low laser power, thus demonstrating that LG_{33} beams would be compatible with this aspect of current gravitational wave detector technology. However, we wish to investigate the effects of a higher power beam on the efficacy of the linear mode cleaner (LMC) with LG_{33} beams.

1. *Designing the Linear Mode Cleaner*

To determine the optimal geometric properties of the linear mode cleaner, it is necessary to find the length at which the incoming beam reflects off both mirrors to reproduce the same beam profile. The first mirror off of which the incoming beam reflects (M1 in (b) of Figure 17) should match the radius of curvature of our (ideally) spherical beam. Instead of matching a mirror to the beam, it is more efficient to adjust the cavity length, and thereby the radius of curvature, to match the beam to the mirror, for there is a large range of mirrors commercially available from which to chose. Thus, with the beam waist position aligned with the entry point of the cavity ("0"), the radius of curvature will be infinity at the second mirror reflection (M2), allowing the LG_{33} modes to become resonant.

$$R(z) = z - z_0 + \frac{z_R^2}{z - z_0} \tag{17}$$

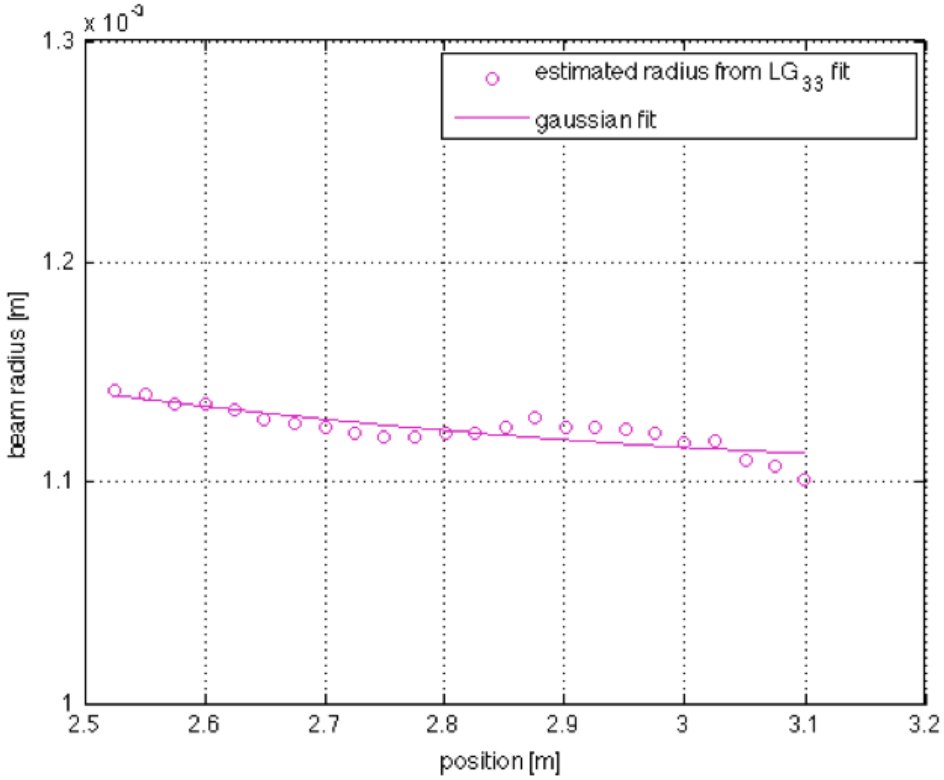

FIG. 16. Beam size of the DOE output beam. The calculated beam waist and position are ω_0= 1113 μm and z_0 = 3.36 m.

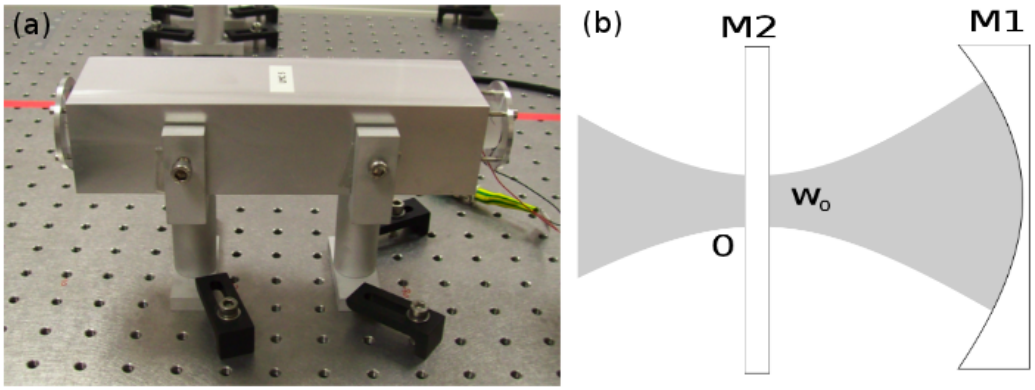

FIG. 17. The linear mode cleaner (a) manufactured and installed on the Birmingham table top and (b) diagram of entering beam. The flat mirror and curved mirror (radius of curvature of 1 m) are mounted on the 21 cm aluminum spacer. M1 is the mirror off of which the beam first reflects. M2 is the second mirror. 0 marks the beam's entry point into the cavity, as well as the location of the beam waist, ω_0

Evaluating Equation 17 for a ROC of infinity and length L equal to z - z_0, one obtains the characteristic expression

$$0 = -LL_0 + L^2 + z_R^2. \tag{18}$$

From this expression, the optimal length of the LMC cavity was determined to be 21 cm for our specific wavelength and beam waist. Using Equation 18 and the Rayleigh range, one can solve for the beam waist at input mirror of the

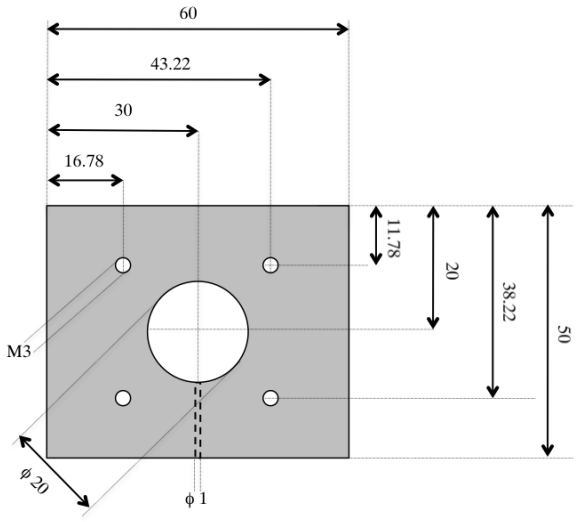

FIG. 18. Facial dimensions of the spacer in cm, with a length of 21 cm. The center hole is the actual cavity, while the square of four holes are for four mounting screws.

LMC the and get

$$w_0 = ((L_0 - L)L)^{\frac{1}{4}} \left(\frac{\lambda}{\pi}\right)^{\frac{1}{2}} \tag{19}$$

Figure 19 is a plot of this calculated waist versus the length of the LMC, giving us an idea of what the beam profile looks like within the cavity. An aluminum spacer of the dimensions shown in Figure 18 was manufactured, then cleaned in an ultrasonic bath of distilled water. A set of mirrors (one flat with reflectivity about 98% and one curved with a radius of curvature of 1 m and similar reflectivity) were then mounted on the ends of the spacer. To lock the cavity (described below), a Piezo-electric transducer (PZT) is installed between the spacer and M1.

2. Mode Matching for the LMC

The linear mode cleaner in our setup required a 370 μ beam waist. To achieve this, it was necessary to install two more mirrors in our setup, BL03 and BL04, after a string of turning mirrors used to remain within the geometrical confines of the available space in Hanover. JamMt was used to determine what focal lengths of these two new lenses would produce the desired beam parameters. This simulation work indicated that both BL03 and BL04 should be converging lenses with focal lengths of 203 mm. The optimal positions of BL03 and BL04, for the LMC requirements were determined using the same ABCD matrix method as described in sections II C 2. By changing the necessary parameters to our ABCD matrix Matlab script, plots similar to Figures 7,8,9, and 10 were created and used to determine lens positions. Again, these calculations were compared with the simulation tool JamMt.
Several sets of data were taken in the processes of aligning BL03 and BL04 in search of the optimal beam waist size and position. The data was analyzed in the manner described above. Once satisfied with the beam waist and position exiting BL04, four more turning mirrors, BM07 − BM10, were installed to move the beam along the appropriate distance to suit the geometry of the table setup and beam waist position. Measurements were taken to ensure the output beam matched the desired beam parameters of 370 μm at an appropriate distance on the table. The fitting script was then run to determine the quality of the beam. Several micrometer adjustments to the position of BL04 yielded an acceptable beam. Figure 20 shows the calculated beam profiles after each adjustment BL04, where it easy to see the affect of each millimeter movement on the beam waist and position. The position of the last two turning mirrors before the LMC allows for increased precision in beam alignment upon the first lens of the LMC without seriously affecting the quality of beam waist size.
To better fit the table space while matching the beam waist position, BM09 and BM10 were repositioned so that the LMC could be installed in a more advantageous position. The results of aligning the mirrors and another millimeter adjustment to BL04 are shown in Figure 21, the final beam profile of the beam that enters the LMC. The beam, with a waist of 382.3 μm, is suitably close to the desired 370 μm for this stage of the experiment. Since the beam waist

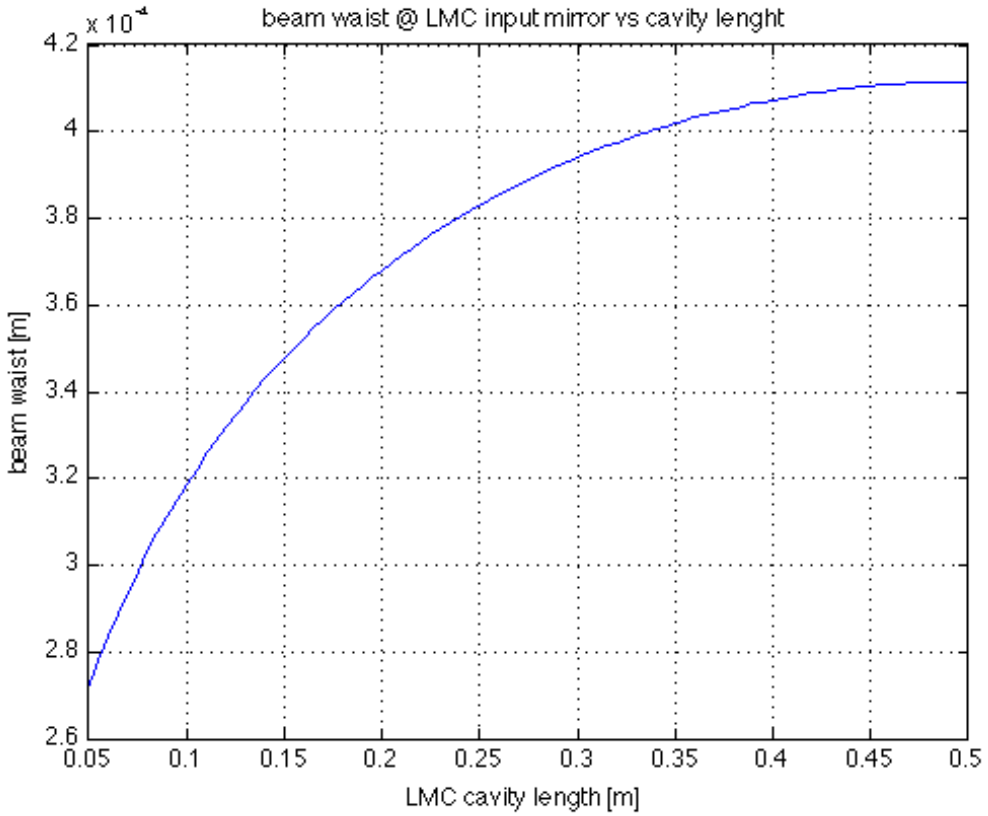

FIG. 19. Beam profile calculated from the beam waist at input mirror of the LMC from Equation 19 plotted against the LMC length.

position is at 5.3511 m, the entry point of the linear mode cleaner must be placed as close as possible to that position (M2 in (b) of Figure 17).

F. First Installation and Locking of the Mode Cleaner

The linear mode cleaner was installed with the entry point located near the 5.35 m beam waist position. A beam splitter was placed after the exit point of the LMC, where the transmitted light can then be analyzed at two ports created by a beam splitter: a photodiode and a CCD camera, as seen in Figure 22. (To converge the beam onto the photodiode, a lens was place between the detector and beam splitter.) A schematic of the electronics setup is shown in Figure 23 while Figure 24 is a photo of the electronics in the lab. In Figure 26 we show the beam transmitted by the LMC with the cavity locked. The LG_{33} mode is visibly cleaner than those just after the DOE, like the samples shown in Figure 15.

III. CONCLUSION

The Birmingham IFO group's 1064 nm laser was successfully transformed after a set of lenses (BM-A and BM-B) to the beam to match the parameters of the Hanover laser (547 μm beam waist). The fundamental beam passed through two more lenses (BL01 and BL02) to create a large (3.5 mm radius), well collimated beam. The beam was then transmitted through a diffractive optical element which imprints the LG_{33} mode upon the beam. Two more lenses (BL03 and BL04) focused the beam for optimal waist size (370 μm) for the linear mode cleaner. The setup in the Birmingham lab is ready to characterize the manufactured LMC with old and new mirrors to investigate LMC use with LG_{33} modes at low laser power. After these characterizations, the setup will be ready to install on the Hanover Advanced group's table and be tested with the 200 W laser.

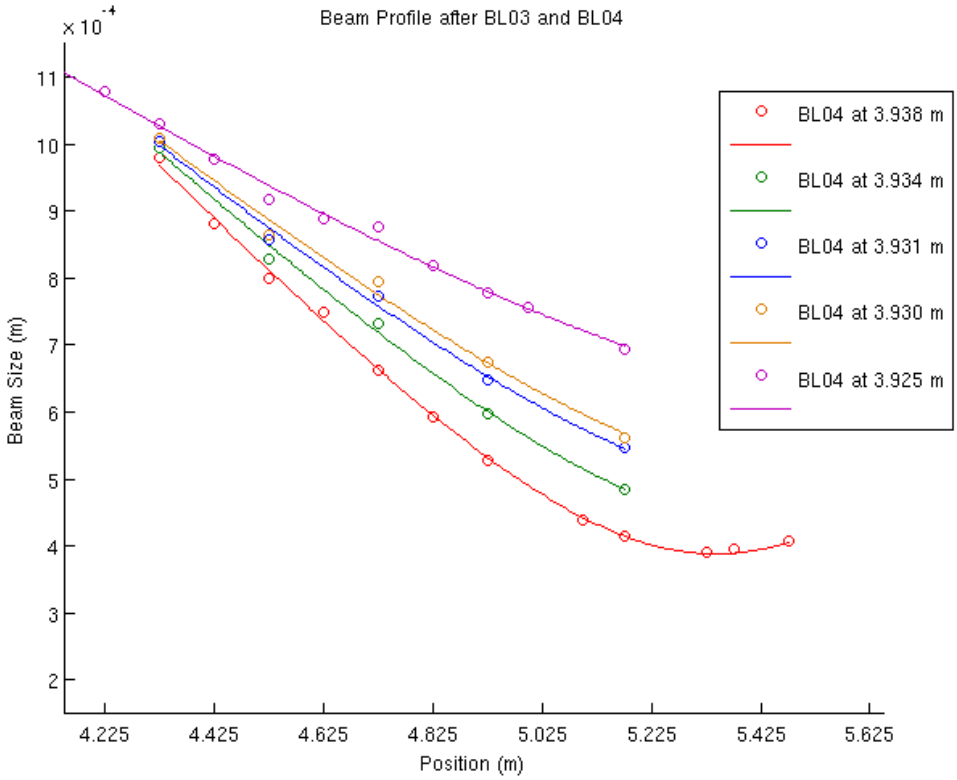

FIG. 20. Beam profiles after BL04 for a series of alignment adjustments. Millimeter adjustments to the position of BL04 dramatically affect the beam waist size and position.

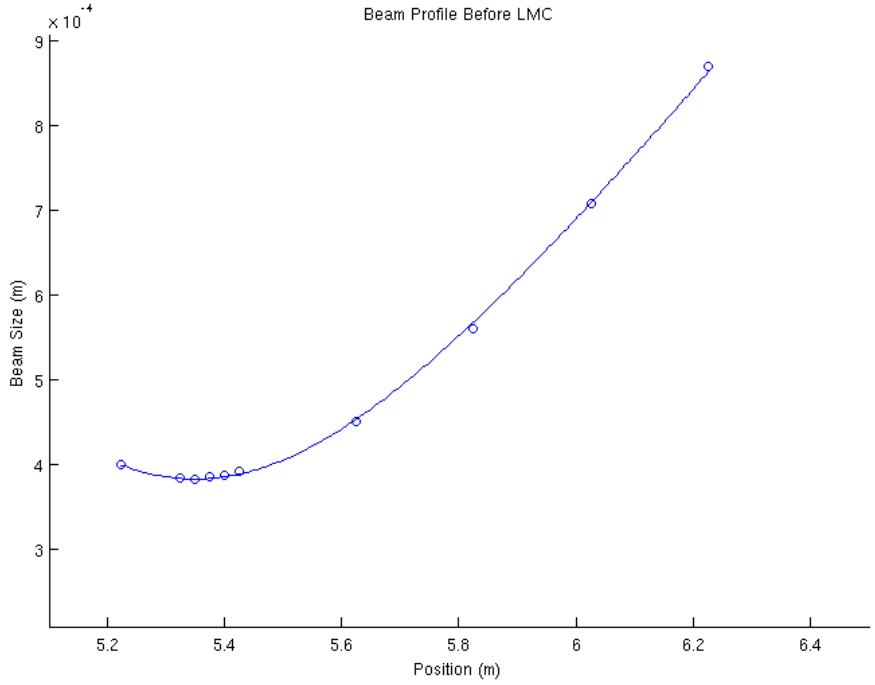

FIG. 21. Beam profile of the beam incident upon the LMC. The calculated beam waist and position are for the beam are ω_0= 382.3 μ and z_0 = 5.3511 m.

ACKNOWLEDGMENTS

This research was made possible by the National Science Foundation Research Experience for Undergraduates grant PHY-1005036, University of Florida Department of Physics and Astronomy, and the University of Birmingham Department of Physics and Astronomy Interferometry Gravitational Wave group, headed by Andreas Freise. Thanks to Paul Fulda and Mengyao Wang for their direction and guidance in the lab, but especially to Ludovico Carbone, without whose instruction and patience this project would not have been possible.

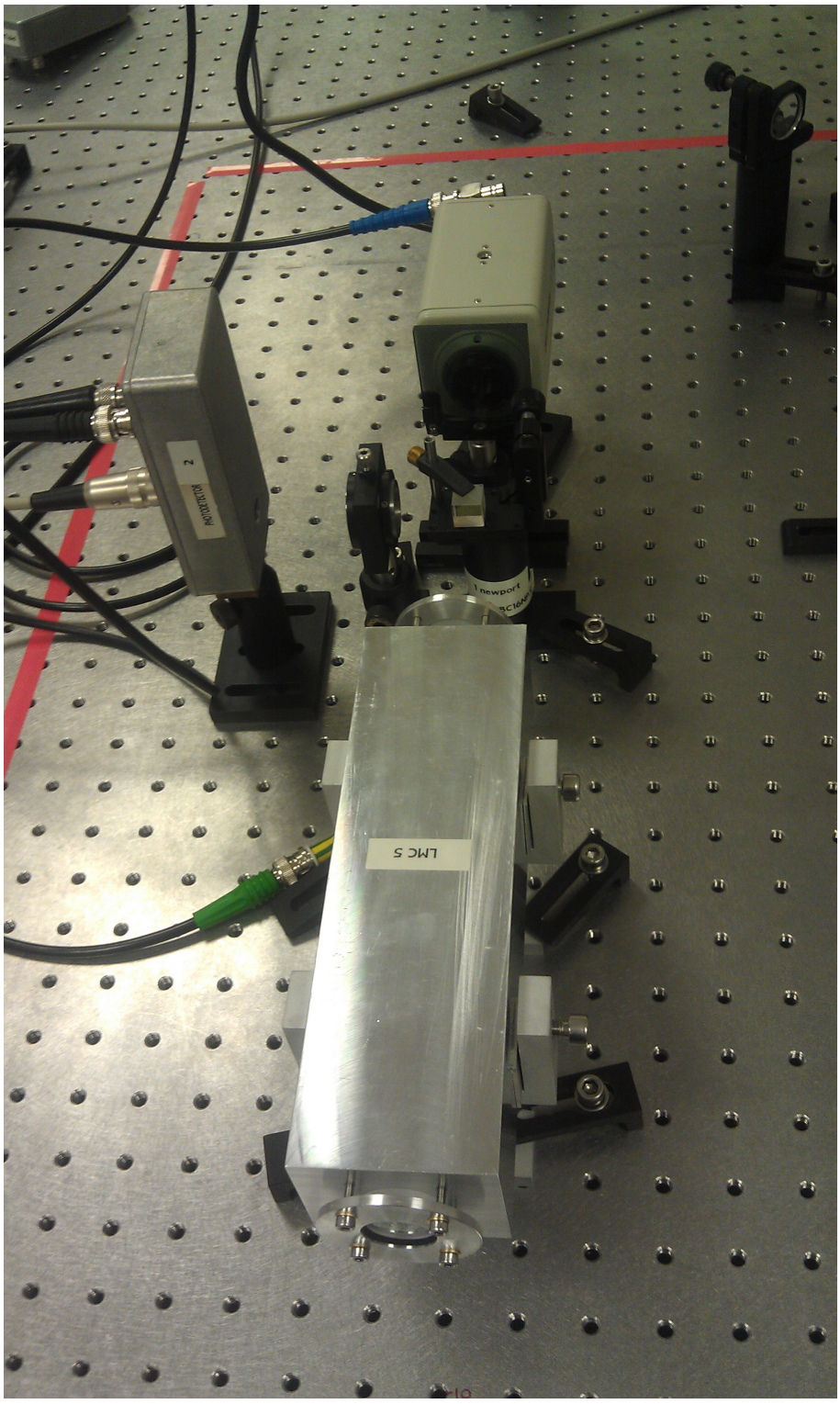

FIG. 22. Photo of the beam analysis setup including the LMC, beam splitter, CCD, lens, and photodiode.

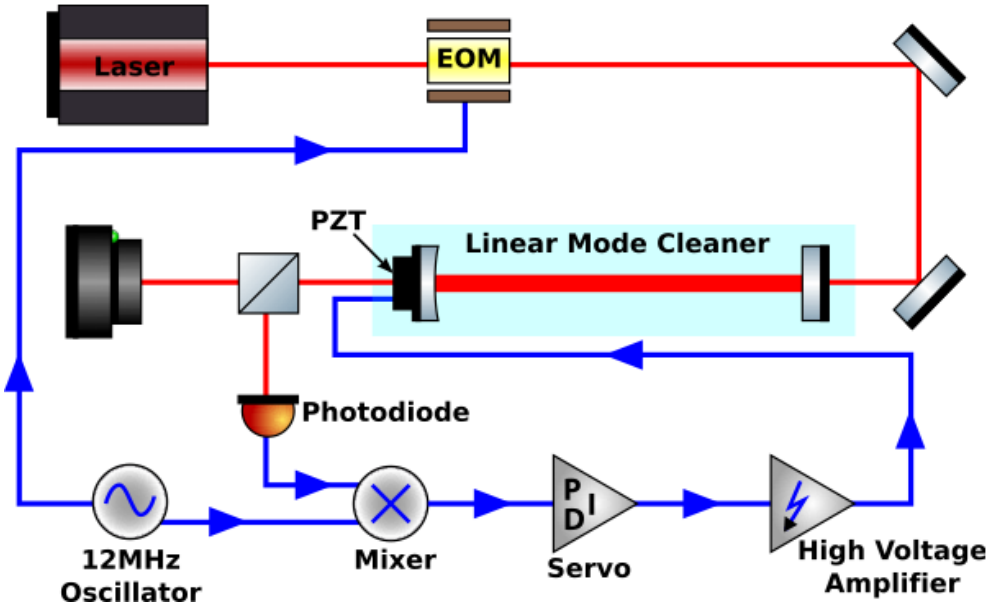

FIG. 23. Schematic of the electronics setup in the Birmingham experiment.

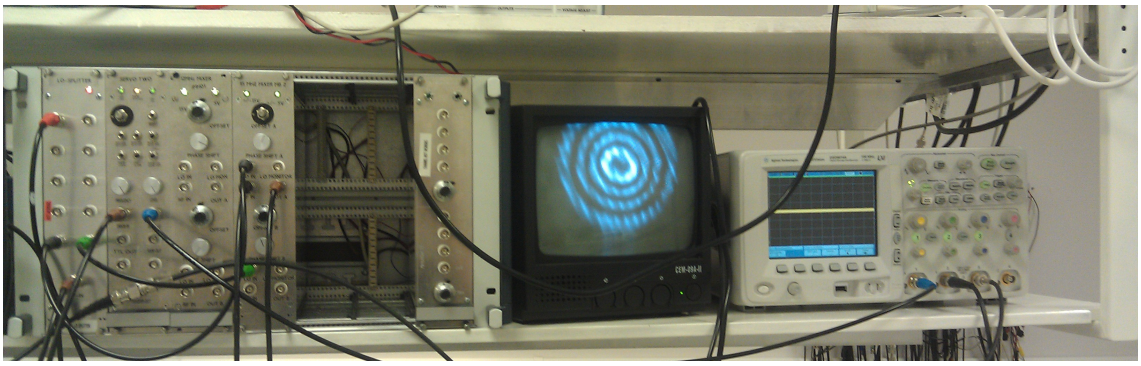

FIG. 24. . Photo of electronics setup. On the left is the rack containing the mixer, servo, and high voltage amplifier used to create the feedback signal. Next is the monitor connected to a CCD camera where in this photo the locked mode of the LG_{33} beam is visible. On the right is oscilloscope used to monitor the photodiode signal.

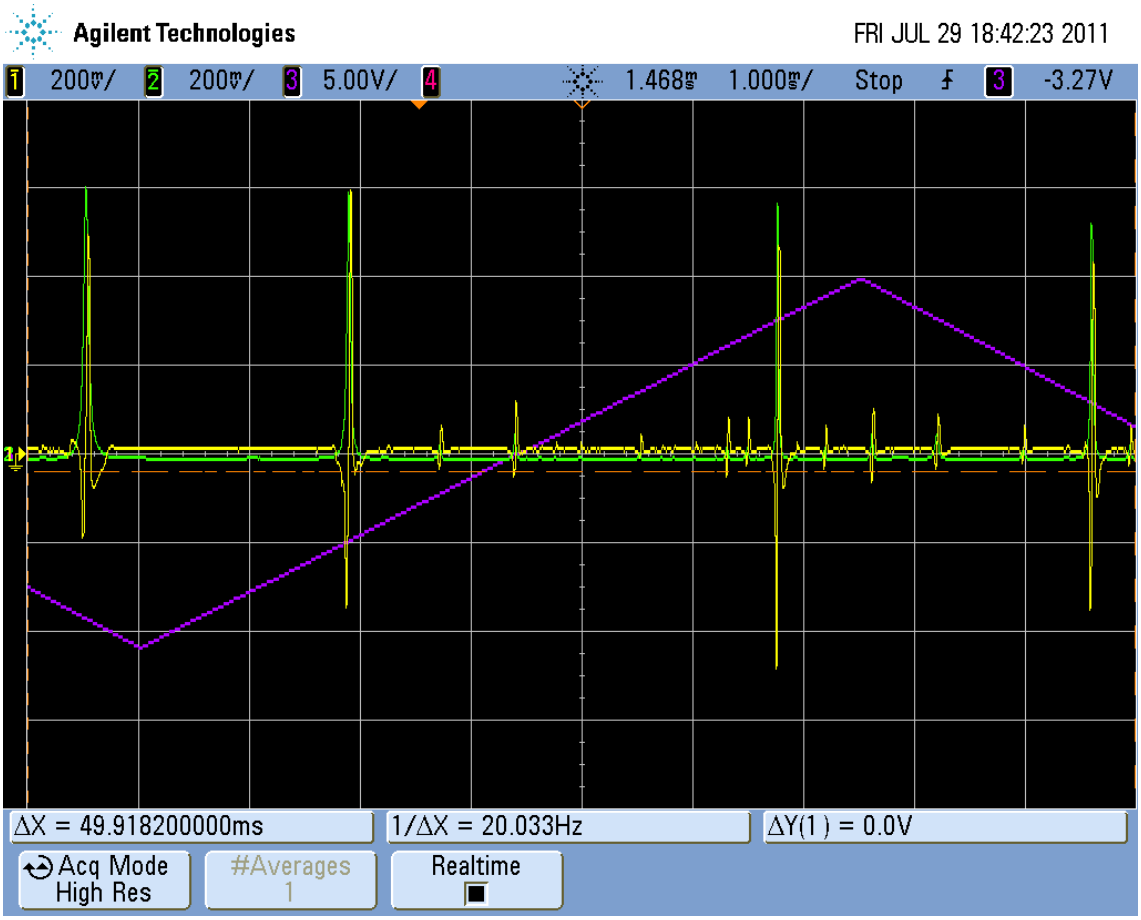

FIG. 25. Sample of signals observed on the oscilloscope. The purple curve is the scanning signal applied to the PZT. The green curve is the intensity of light incident upon the photodiode. The yellow curve is the error signal constructed from the superposition of the 12 MHz-mixed photodiode signal and the EOM driving oscillating signal. The error curve is used to feedback into the control loop of Figure 23 and lock the cavity.

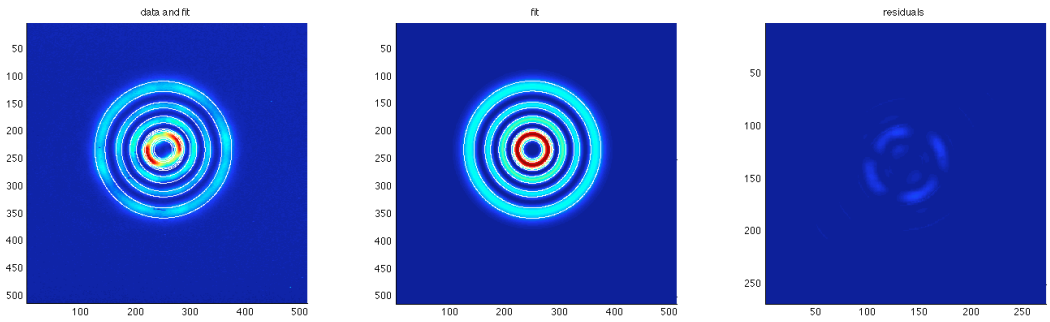

FIG. 26. Beam profile of the locked cavity. The beam waist was calculated to be 559.3 μm.

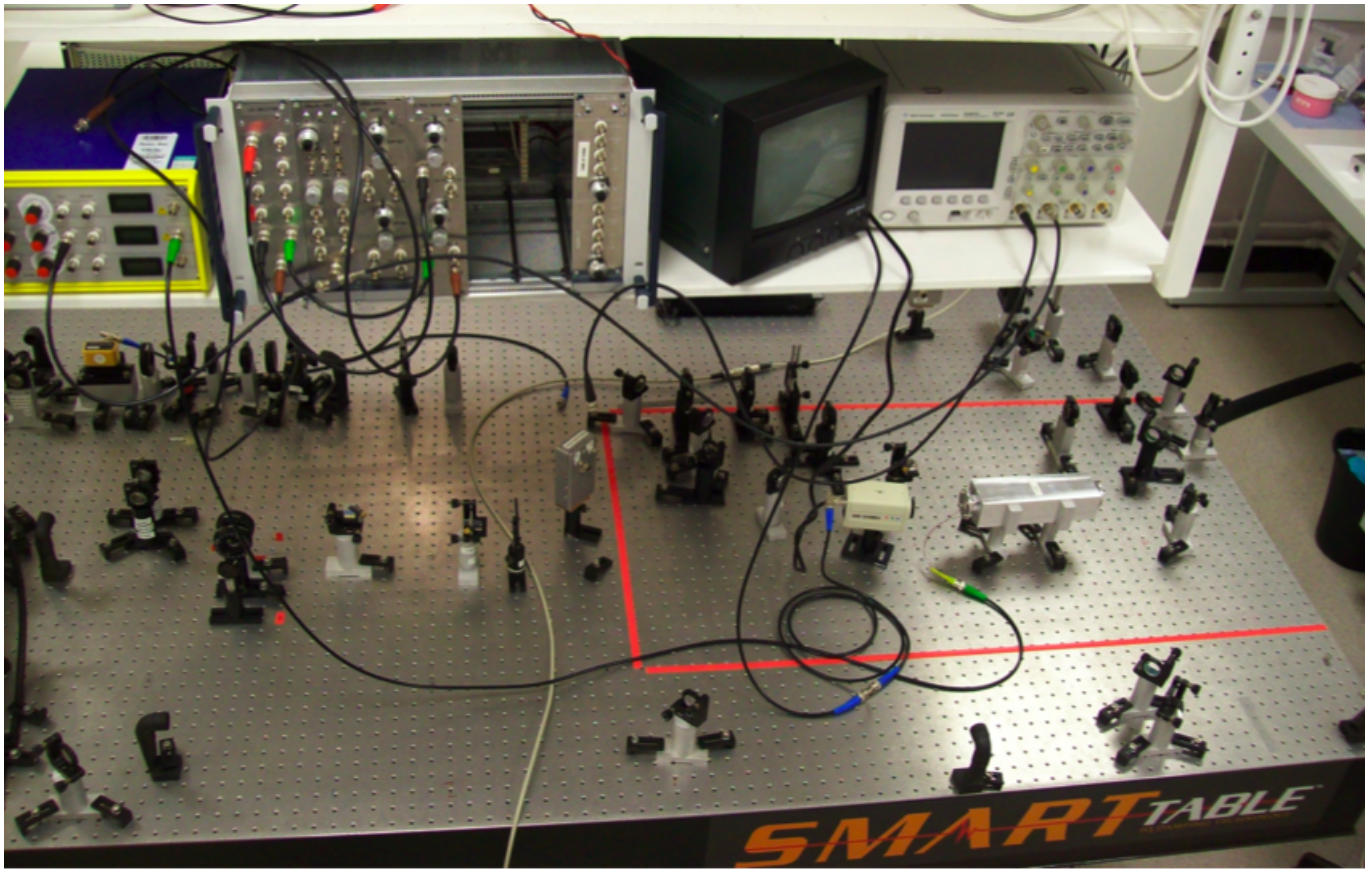

FIG. 27. Photo of the Birmingham table top setup.

[1] Alex Abramovici, William E. Althouse, Ronald W. P. Drever, Yekta Grsel, Seiji Kawamura, Frederick J. Raab, David Shoemaker, Lisa Sievers, Robert E. Spero, Kip S. Thorne, Rochus E. Vogt, Rainer Weiss, Stanley E. Whitcomb, and Michael E. Zucker. Ligo: The laser interferometer gravitational-wave observatory. *Science*, 256(5055):325–333, 1992.

[2] Sheila Rowan Jim Hough Matthew Pitkin, Stuart Reid. Gravitational wave detection by interferometry (ground and space). *Living Reviews in Relativity*, 14(5), 2011.

[3] Benot Mours, Edwige Tournefier, and Jean-Yves Vinet. Thermal noise reduction in interferometric gravitational wave antennas: using high order tem modes. *Classical and Quantum Gravity*, 23(20):5777, 2006.

[4] Jean-Yves Vinet. On special optical modes and thermal issues in advanced gravitational wave interferometric detectors. *Living Reviews in Relativity*, 12(5), 2009.

[5] Paul Fulda, Keiko Kokeyama, Simon Chelkowski, and Andreas Freise. Experimental demonstration of higher-order laguerre-gauss mode interferometry. *Phys. Rev. D*, 82(1):012002, Jul 2010.

[6] B. Wilke. Stabilized lasers for advanced gravitational wave detectors. *Laser Photonics Reviews*, 4:780–794, Nov 2010.

[7] Kenneth Strain Andreas Freise. Interferometer techniques for gravitational-wave detection. *Living Reviews in Relativity*, 13(1), 2010.

[8] Sharon A. Kennedy, Matthew J. Szabo, Hilary Teslow, James Z. Porterfield, and E. R. I. Abraham. Creation of laguerre-gaussian laser modes using diffractive optics. *Phys. Rev. A*, 66(4):043801, Oct 2002.